Compton Scattering in Aluminum

Dawit Belayneh
(Dated: February 2020)

In this report we present the results of our Compton scattering experiment in which we scatter Cs-137 photons with an Aluminum rod at an initial energy of $662[Kev]$. The main goal of the experiment is to test if the angular dependence of the scattered photon energies matches the theoretical expected values given by Compton's formula.

I. THEORY

Compton Scattering [1], is a process by which a photon scatters off of a free or weakly bound electron in the regime where the photon energy is much larger than the binding energy of the electron. Compton's formula predicts the angular dependence of scattered photons as a function of the rest energy of the electron m_0c^2 and the incident energy E_γ of the photon. For a scattered photon making an angle of θ degrees with the original photon path we predict that the final energy of the photon is given by:

$$\boxed{E_{\gamma'} = \frac{m_0c^2}{1 - \cos\theta + (m_0c^2/E_\gamma)}}$$

II. EXPERIMENTAL SETUP

To measure scattered photons we setup our experiment as follows. A Photo-Multiplier Tube was attached to a NaI scintillator with lead shielding. The electrical outputs from the PMT were directed to a Pulse Height Analyzer which produced count spectra of detected events. The NaI + PMT detector was placed on an angular rail which was located at a fixed radial distance from a one inch diameter Aluminum rod placed on an angle scale between our detector and Cs-137 source. The Cs-137 source was shielded and fixed in place. A variety of additional radioactive sources were utilized other than Cs for calibration purposes.

III. DATA COLLECTION REQUESTS

We submitted two data collection requests to our lab staff who performed the data collection.

In the first request we asked for spectra produced by Na-22 and Ba-133 sources placed at 0 degrees with respect to our detector with the Aluminum rod removed. The rational behind choosing Na-22 and Ba-133 was so we can access data points both on the lower and upper end of our detector channel range. Specifically we intended to use the $81,356[Kev]$ decay lines of Ba-133 and the $511,1270[Kev]$ decay lines of Na-22. Additionally, we requested data to be taken with the Cs-137 source where the detector was placed in angles ranging from $0-170$ degrees, every 10 degrees. Due to the limitations of our setup we were only able to receive data up to 120 degrees. A step size of 10 degrees was chosen after qualitatively examining the curve produced by Compton's formula so as to test qualitatively different areas of the curve. We also requested various dimensions of parts in the experiment. This was done so we could estimate the effective size of our Aluminum rod as seen from the source and detector.

After some preliminary analysis of the first data batch, we determined to request further data for calibration. Thus, we requested the energy spectra of Cs-137, Co-67, Co-57, and Am-241 at 0 degrees with respect to our detector and Aluminum rod removed. This was done so as to make our calibration more precise. However, we only used the Na-22 and Ba-133 sources for our calibration analysis as we did not see much improvement after adding data from the new sources.

IV. DATA ANALYSIS

We collected two sets of data which we will refer to as calibration and angle data. The calibration data was used to calibrate the channel readings coming out our detector to energy values while the angle data was used to test the scattering formula discussed above. In what follows we discuss the conditions under which the data were collected and the details of the data analysis performed on the raw data to extract the relevant quantities.

A. Calibration Data

Our NaI + PMT detector setup does not directly measure the energies of the photons striking it. Instead, energy readings are reported as counts on a corresponding channel number. The energy of a photon and the corresponding channel number it is counted under are linear functions of each other. That is:

$$\boxed{E(c) = mc + b}$$

where E is the energy and c is the channel number. We would like to measure the values of the calibration slope m and calibration intercept b.

1. Collection Settings

To achieve this goal we collected the spectra of photons coming of multiple photon sources with varying prominent decay energies. We looked at Na-22 at energy of $511[Kev]$ and Ba-133 at energies of $81, 356[Kev]$. This gave us three data points to fit a linear function to with good energy range.

Both sources were placed right at the lip of our detector with the detector turned at 90 degrees from the closed Cs-137 source. This was done because our setup does not allow for the Cs source to be fully removed. The presence of the closed Cs source is felt in the spectrum of the other sources as we will see shortly. The gain on our PHA was set such that the $662[Kev]$ peak from Cs-137 would be close to the right edge of our channel range. This resulted in the Na-22 $1.27[Mev]$ peak being outside our channel range.

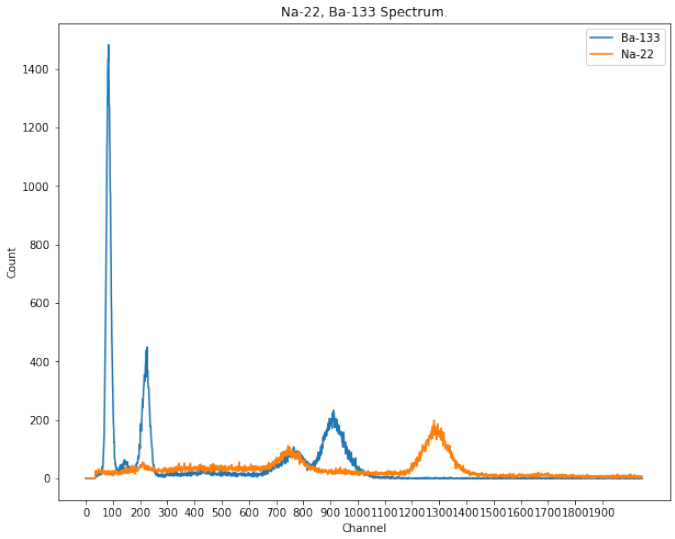

FIG. 1. Na-22, Ba-133 calibration data.

2. Analysis

Next we identified the peaks on our spectra with the corresponding decay lines of the sources, thereby assigning a known energy value to the peaks. Our Na-22 and Ba-133 spectra contained a Gaussian in the common channel range of 600 to 800. This Gaussian had a peak count of around 100. Since these sources do not share a common decay energy we were able to identify this as a systematic source of error coming from the closed Cs-137 source at 90 degrees from the detector.

To further confirm our identification we computed the predicted final energy of a Cs photon at an energy of 662 [Kev] scattering at an angle of 90 degrees using Compton's formula. Using preliminary values for our calibration constants we found that we should see a peak centered at around channel number 750 which matches the location of the common peak as can be seen in Figure-1.

Returning to our main purpose of measuring the calibration constants, we then extracted the peaks of our interest by applying a cut window on the channel numbers. This was done by inspection so as to include relevant features of the peak and obtain best possible fit. We then performed a least chi-squared fit of the peaks to a Gaussian function with a linear background to account for the effects of Compton shelves and other backgrounds. We retained fits with reduced chi-squared values close to 1, as shown in Figure-2.

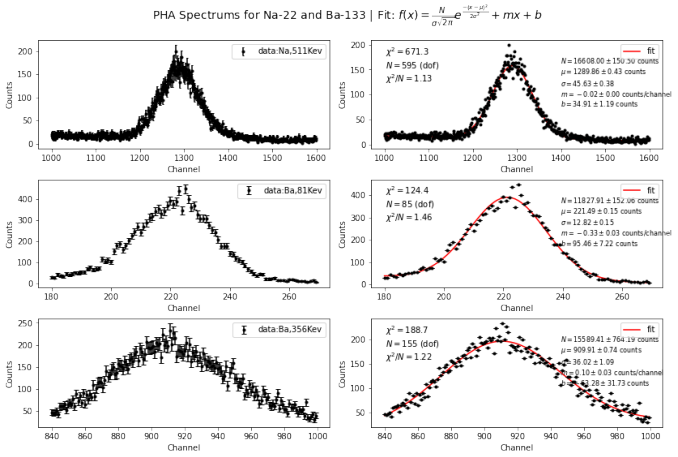

FIG. 2. Na-22, Ba-133 peaks with standard counting errors and fits.

We extracted the channel numbers of the centers of the peaks which correspond to the energy of the most common decay line of the corresponding sources. Table-1 summarizes the results with their fit uncertainty. We then used these values to perform a linear fit on the data points (E, C), where E is the known decay energies and c is the corresponding channels. The results are summarised in Figure-3.

Source	$E_\gamma[Kev]$	C	ΔC
Ba-133	81	221.49	0.15
Ba-133	356	36.02	1.09
Na-22	511	45.63	0.38

TABLE I. Channel numbers of peaks and their error as obtained from a Gaussian fit. Here, C is the channel number of the center of the peak and E_γ is the energy of photons from source.

Notice that the line in Figure-3 gives us the relation $C = \alpha E + \beta$. We can express the energy as a function of channel numbers by inverting this equation.

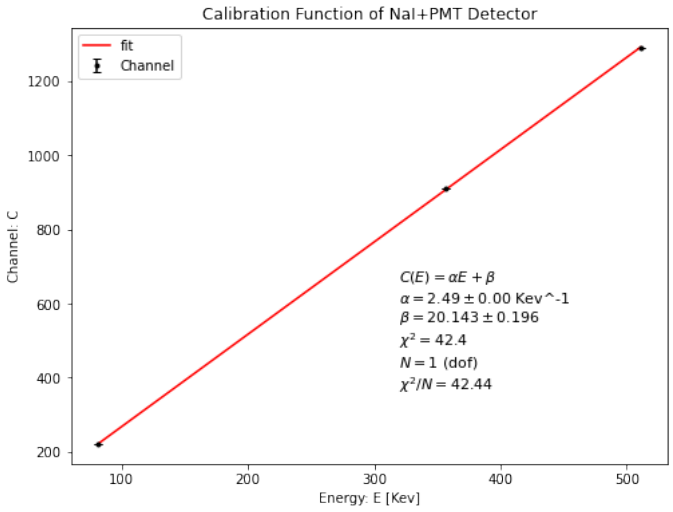

FIG. 3. Linear dependence of channel number and energy inside our detector.

3. *Calibration Uncertainty and Final Results*

The percentage error in the calibration slope is given by:

$$\frac{\Delta m}{m} = \frac{\Delta \alpha}{\alpha} = 0.02\%.$$

The percentage error in the calibration intercept is given by:

$$\frac{\Delta b}{b} = \sqrt{(\frac{\Delta \alpha}{\alpha})^2 + (\frac{\Delta \beta}{\beta})^2} = 1\%.$$

Our final results are:

$$\boxed{m = (0.40 \pm 0.00)[Kev]}$$

$$\boxed{b = (-8.01 \pm 0.08)[Kev]}$$

B. Angle Data

To test the Compton scattering formula we needed to measure the energy of scattered photons coming out of our Cs-137 source at various angles. Once we measured the final energy of the photons at a given angle we compared it to the predicted energy as calculated by the scattering formula.

1. *Collection Settings*

To measure the final energies of the scattered photons, we collected data at angles ranging from 0 to 120 degrees,

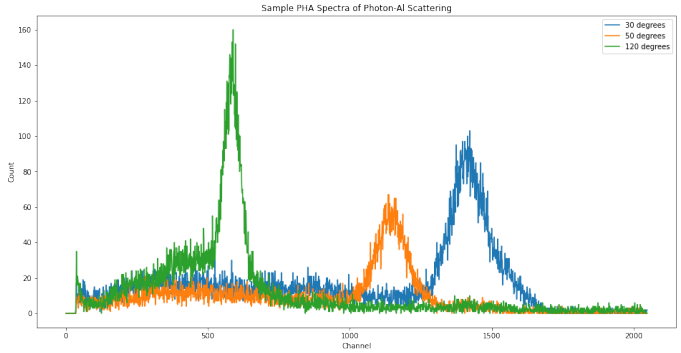

FIG. 4. Sample spectra of photons scattering at 30, 50, 120 degrees.

every 10 degrees. This was achieved by rotating the detector on the angular rail by the required angle. The gain on our PHA was kept as when calibration data was collected, so that the 0 degree peak at $662[Kev]$ was close to the right of our channel range. For each angle, the corresponding raw data contained a single prominent peak as well as a Compton shelf, Compton Edge and Backscattering events. Figure-4 shows some sample spectra.

2. *Analysis*

Since our angle data contained a single peak for each angle, peak identification was not needed. We extracted each peak by applying a cut window on the channel numbers. This was done by inspection so as to include relevant features of the peak and obtain best possible fit. In retrospect, we understand that our data is not clean enough to perform satisfactory fits on some angle spectra, specifically, angles in the 10 to 60 degrees range. We were thus forced to use a stringent cut window which left out a portion of our Gaussian.

In Figure-5, if we compare the window size used on the 50 degrees spectra with the window size used on the 120 degrees spectra, we see that we had to leave out a portion of 50 degrees Gaussian on its left side to achieve a fit comparable to the 120 degrees one. As an indication of the high level noise contained in the data, a very small increase in the window size to the left of the 50 degrees peak caused our fit to converge not to the clear Gaussian but a local minimum. If the data was clean, we would expect the fit to be stable under such changes. The same instability was the case for all angles in the range 0 to 60 degrees. This is a result of our failure to perform sufficient background subtraction.

After extracting the best Gaussian fit we could from the data, we then extracted the center channel numbers for each degree. These channels correspond to the final energy of the scattered photons at a given angle.

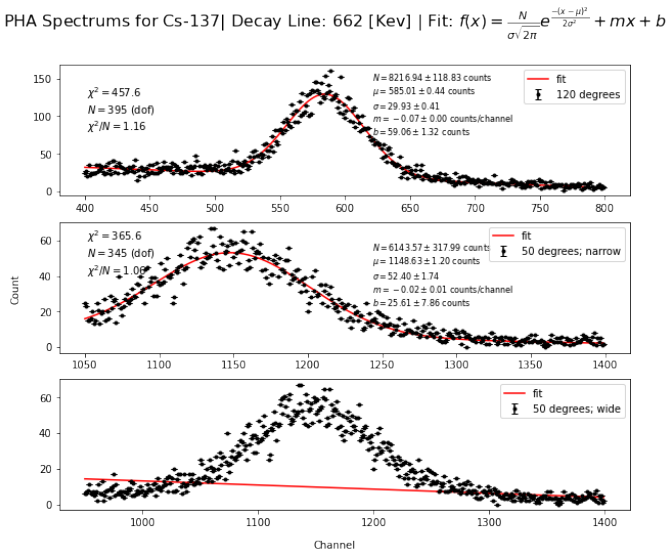

FIG. 5. Sample fits of angular peaks at 50 and 120 degrees. The wide cut 50 degree fit illustrates the low quality of data.

3. *Angle Uncertainty*

The error on our angle measurements comes from two significant sources: the resolution of our angle scale and the fact that the Al rod is an extended object. The former error is known to be 1 degrees.

The fact that our Al rod is not a point particle causes it to have different effective size as seen from the source and the detector. To illustrate the error that arises as a result consider and equal height slice of our experimental setup at eye level of the detector and source. Figure-6 is a simplified diagram of the geometry that arises.

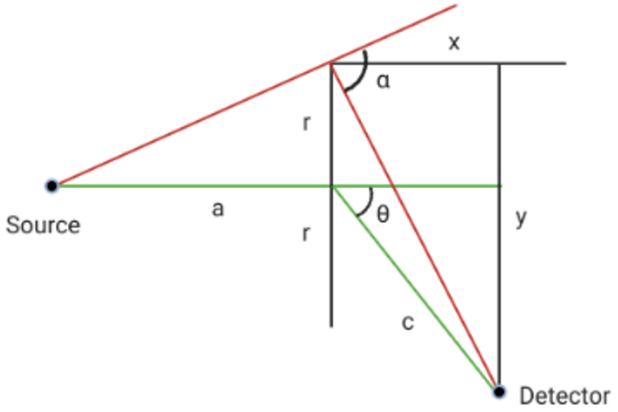

FIG. 6. Equal height slice of our experimental setup at an elevation of detector and source eye levels.

In Figure-6 r is the effective radius of the Al rod. This will be calculated below. The green path is a path a photon would take if it scattered right at the center of our Al rod. The outgoing line makes an angle of θ degrees with the original path. In the diagram $\theta \in [0, 90]$ degrees. The red line is the path a photon would take if it scattered right at the edge of the effective size of the Al rod. We would like to see by how much this new scattering angle is from the ideal green one. The difference will be an estimation of our error. Finally, a is the radial arm from the Al rod to the source and c is the radial arm from the Al rod to the detector.

We have that $x = c\cos\theta$ and $y = r + c\sin\theta$. Then, it is straightforward to compute the new scattering angle which will be

$$\boxed{\alpha = \arctan\frac{r}{a} + \arctan(\tan\theta + \frac{r}{c\cos\theta}).}$$

Thus, we estimate the error in measuring the angle $\theta \in [0, 90)$ degrees to be given by:

$$\boxed{\Delta\theta = 1 + \|\alpha - \theta\|}$$

degrees, where the 1 comes from our angle scare resolution. We note that this formula only holds for the specified range.

To compute the effective radius of the Al rod, we have to compare the actual radius with the radius as seen from the source and the detector. The experimental effective radius then becomes the smallest of the three values. To compute the effective radius of the Al as seen from the source/detector is another simple geometry problem. To illustrate the computation we will compute the radius as seen from the source.

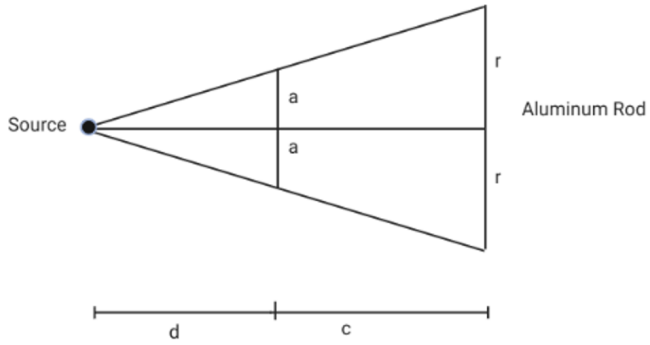

FIG. 7. An equal slice of experimental setup at source eye level. The source is placed inside a lead shielding with a circular opening.

In Figure-7, d is the distance from the source located inside a lead shielding to the face of the lead shield. c is the distance from the face of the lead shield to the Al rod. r is the radius of the Al rod as seen by the source. a is the radius of the eye of the lead shield. We see that source can only output photons inside the cone of base radius a and height d. Thus, the source sees the Al rod

at an effective radius. By the similarity of the triangles above we can deduce that,

$$\boxed{r = \frac{a(c+d)}{d}.}$$

As seen from	Effective Radius
Source	1.30 cm
Detector	10.32 cm
Al-rod	1.27 cm

TABLE II. Effective radius of Al-rod as seen from detector, source and Al-rod itself.

Table 2 summarizes the three radii calculated by this method. Even though there is a small error in our length measurements we ignore them as they are not significant enough to affect our angular error. We see the our experiment's effective radius is given by the actual Al rod radius as it is the smallest one.

Finally, as an illustration of the error calculation, we can calculate the deviation expected at 90 degrees as follows. From Figure 6, it is clear that $\Delta\theta = \arctan\frac{r}{a}$ degrees when $\theta = 90$ degrees. Thus, $\Delta(\theta = 90) = 1 + 1.51 = 2.51$ degrees. A similar computation was performed on all measured angles to arrive at an estimate of the angle error.

We would like to point out that this is a simplified estimation of the angle error, as not only does radius of the Al rod change as seen from the source/detector but so does its height. Thus, just like there is an effective Al radius we also have an effective Al height. However, we ignore this distortion under the assumption that it will not affect the result significantly. Furthermore, there are errors that arise from photons double scattering inside the Al rod. We again ignore this error on the justification that the probability of double scattering is low.

4. Energy Uncertainty

The uncertainty in the final measured energy for each angle comes from two main sources: the error in our calibration constants and the error in the center of the energy peak coming from our fit. The absolute error in the error is then,

$$\Delta E = \sqrt{(\Delta mc)^2 + (\Delta b)^2} = \sqrt{m(\Delta c)^2 + (\Delta b)^2},$$

where m, b are the calibration slope and intercept and c is the channel number. The last equality is justified by the fact that the error $\Delta(mc)$ is dominated by Δc for all our angle measurements.

The noise in our data is a significant source of error as discussed in the analysis section. This noise is likely background radiation picked up by our detectors. However, because we do not have a handle on the size of the noise we can not estimate it consistently for all angle values. We therefore make the assumption that the background noise is contained in our center channel errors with the understanding that they are a sizable underestimation of the actual error.

V. FINAL RESULT AND DISCUSSION

Our final energies showed good agreement with the predicted energies of Compton's formula. Qualitatively, as Figure-9 shows, most of our measured points are on the theoretical curve. However, as Figure-8 shows, none of the predicted energies are within our energy errors. The typical measurement error is around 0.02% while most predicted values have a disagreement of around $1 - 3\%$ with the measured values. As we mentioned in the analysis section, we take this to mean that we have significantly underestimated our energy errors. We expect that better background subtraction can be employed to get better agreement with our data. One way to achieve this is to collect readings for each angle with our source closed and the Al rod removed. These counts can then be subtracted from the scattering data.

Angle [deg]	Angle Error [deg]	E [Kev]	E Error [Kev]	Predicted E [Kev]
0	4.49	647.48	0.10	662.00
10	4.45	633.09	0.19	649.22
20	4.35	611.41	0.18	614.03
30	4.19	564.59	0.41	564.10
40	3.99	509.82	0.36	508.02
50	3.75	453.82	0.49	452.57
60	3.47	403.66	0.44	401.76
70	3.17	358.79	0.30	357.37
80	2.84	321.76	0.36	319.72
90	2.51	290.67	0.33	288.39
100	2.18	266.77	0.28	262.65
110	1.86	243.01	0.16	241.73
120	1.55	227.16	0.20	224.92

FIG. 8. Final result of energy measurements and corresponding errors.

Coming back to Figure-9, we see that angle values of 0 and 10 degrees show worse agreements with the theoretical energies than higher angles. While the general ambient background present in our data plays a factor in this, the severity of the disagreement, not seen in the higher angles, leads us to suspect other, non-systematic sources of error in our data. We suspect that since scattered photons at these angles have high energies, they are more likely to leave our detectors without depositing all of their energy. As such, what we measure is an apparent energy that is different from the actual energy by a significant margin. This would explain why the effect is limited to smaller angles.

Comparing our angle errors with our energy errors

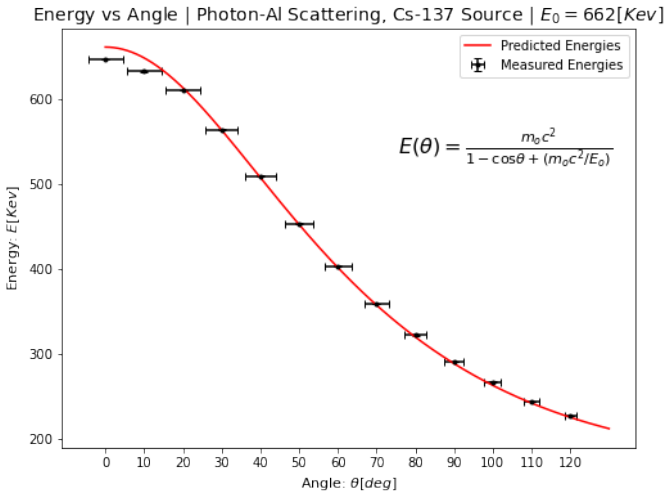

FIG. 9. Final result of energy measurements and corresponding errors.

shows that our angle measurements are the least precise part of our experiment. The errors on our angle measurements range from about $5 - 1$ degrees. This is expected as the Aluminum rod and angle scale have resolutions at a visible scale while count errors tend to be much smaller. Since our angular resolution is not small enough, we can not claim to have rigorously tested Compton's theory in our range of angles. What we can conclude is that our experiment has produced plausible agreement with Compton's formula, especially at the higher angles we examined, where the angular and energy errors are small enough to rule out significant deviations from the theory.

VI. SOURCES

1. Griffiths, David (1987). Introduction to Elementary Particles. Wiley. pp. 17.